C.P. No. 1370

C.P. No. 1370

PROCUREMENT EXECUTIVE, MINISTRY OF DEFENCE

AERONAUTICAL RESEARCH COUNCIL

CURRENT PAPERS

Iterative Calculation of Flow past a Thick Cambered Wing near the Ground

by

C. C. L. Sells

Aerodynamics Dept., R.A.E., Farnborough

LONDON: HER MAJESTY'S STATIONERY OFFICE

1977

£1-75 NET

UDC 533.69.01 : 533.6.044.7 : 533.6.043.1 : 533.682 : 533.6.011.32

*CP No.1370
April 1976

ITERATIVE CALCULATION OF FLOW PAST A THICK CAMBERED WING NEAR THE GROUND

by

C. C. L. Sells

SUMMARY

The author's method to compute the steady low-speed inviscid flow past a wing in free air, is extended to take account of ground effect. The basic method represents the perturbation due to the wing by iteratively computed distributions of sources and doublets on the wing chordal surface; at each iteration the ground effect is represented by the images in the ground plane of these distributions, the strengths of which are calculated from the computed errors in the boundary conditions on upper and lower surfaces. For a given angle of incidence (and Mach number), several heights above the ground in succession can be treated, with some economy in computing time.

Results are presented for a two-dimensional section (RAE 100) and for two variants of a wing of 'airbus' type. Comparisons with another method for the RAE 100 section suggest that the present method generally needs at least three iterations, and that for very accurate results at low ground heights further work on the program is needed.

---

* Replaces RAE Technical Report 76053 - ARC 36856.

CONTENTS

1 INTRODUCTION

In earlier work[1] we have shown how to compute the steady inviscid flow past a thick, cambered and twisted wing (neglecting dihedral) in free air, at low Mach number. The flow field is represented by suitable source and doublet (singularity) distributions in the wing chordal surface, the strengths of which are calculated iteratively by the second-order small-perturbation theory of Weber[2]. A computer subroutine, developed by Ledger[3] and Sells[4], is available to calculate the corresponding flow fields.

In this approach to the problem of a wing in free air, the iterative calculation of the strengths of the singularity distributions is based at each step on finding the amount by which the velocity fields violate the wing boundary conditions of zero normal flow on upper and lower surfaces. For the problem of a wing near the ground, this idea can be extended very simply. The effect of a solid planar ground can be represented by image singularity distributions, and the corresponding interference velocity fields induced on the wing can also be calculated by the Ledger-Sells subroutine and added to the basic velocity fields. The necessary modifications are set out in section 2. The interference fields are expected to be small compared with the basic velocity fields, and the major consequence of this is that they should produce only small perturbations in the boundary-condition errors, which can easily be absorbed into the general error fields to be cancelled (approximately) at each iteration. Thus, no special modification is needed in the program to calculate the successive singularity strengths.

Most of the computer time in this method is needed by the Ledger-Sells integration subroutine, and at first sight it might appear that the additional computation of the interference velocity fields on upper and lower wing surfaces would increase run times by a factor of about three. In fact the penalty is not as large as this, for two reasons. First, since the numerical variation in the interference-velocity integrands subsides rapidly with distance from the singularity plane, the integration (which is adaptive, i.e. compares results for successively larger numbers of function evaluations) takes less time than that for the basic velocity fields. Secondly, the differences between the interference fields on upper and lower surfaces is also expected to be small compared with the basic fields, and indeed may be small compared with the interference fields themselves, so that in most circumstances it should suffice (and this has been assumed in writing the program) to calculate these interference fields

on one surface only. For very accurate work this assumption may fail, as we shall see in section 4 (Results), and then it may be necessary to determine the separate upper- and lower-surface interference fields, perhaps using Taylor series as in Ref.1 (where it was shown how to tackle the similar problem for cambered wings).

The method assumes the planar wake of linear theory, and is therefore less general than that of Maskew[8], who is able to distribute his singularities (vortex rings) over the wing camber surface and one of two possible wake models. However, the results reported by Maskew[8] do suggest that the difference in results, due to different wake models, is often small compared with the difference due to ground effect itself, so we might argue that if we could determine the wake shape as part of the solution, the results would be unlikely to differ much from those obtained with a simple wake model. More significant may be the fact that we can take the thickness interaction into account as well as those of camber, twist and incidence, and in the results section we show a case for which the extra lift generated by ground effect is due principally to changes in the lower-surface pressure distribution, for which the boundary layer is relatively thin, while the upper-surface pressure distribution and its associated thick boundary layer do not change much from their free-air dispositions. This would imply that for this case viscous effects are similar to those for the wing in free air; a result which would be unlikely to emerge from an application of Maskew's thin-wing method. This is an example of the general contention, which we now make, that the inclusion of thickness interactions might allow better prediction of viscous effects.

A possible further advantage of the present method is that, whereas (for one configuration) a panel and matrix method might need up to four times the effort to calculate influence coefficients in the presence of ground effect, compared with the corresponding free-air problem, the present method needs rather less than three times the total effort. When results are required for more than one ground height, the present method can carry over the stored basic velocity field from a previous iteration, thus saving one application of the Ledger-Sells subroutine; but a panel and matrix method can also save time by holding the submatrix of self-induced influence coefficients in store, and it is not easy to predict which method would gain on this point.

The program is written in Fortran and, with arrays dimensioned for a 12×15 collocation grid, requires about 57K words of core store (including about 13K words for a vortex lattice matrix).

2 THE IMAGE SYSTEM IN GROUND EFFECT

We consider a finite wing moving at incidence α and unit speed, parallel to an infinite plane representing the ground. (When the wing is relatively near the ground, departures from parallel motion must be small.) The flow is considered inviscid and irrotational, but may be slightly compressible, even at landing and take-off speeds. We superpose unit velocity on the system in the usual way, so that the wing is considered at rest in a moving airstream, and define cartesian coordinates $(\hat{x},y,\hat{z})$ with origin T_0 at the wing root trailing-edge, with the $\hat{x}$-axis downstream and parallel to the ground, the y-axis to starboard and the $\hat{z}$-axis vertically upwards.

In Ref.1 we considered a wing in free air, with no ground effect, and showed how to calculate the resulting flow field iteratively, following Weber[2]. The perturbation flow field due to the wing is represented by distributions of sources and doublets on the wing chordal surface. To start the iteration, the strengths of these singularities are estimated by linear theory; the resulting velocity fields are computed at certain collocation points on the upper and lower wing surfaces, the errors in the boundary conditions of zero normal flow are determined and combined into symmetrical and antisymmetrical parts, R_t, R_ℓ respectively, and perturbation singularity distributions are generated to cancel these errors approximately, again using linear theory. The cycle can be repeated as often as desired; in practice two or three iterations suffice for acceptable convergence.

When the wing chordal surface is non-planar, we consider a plane parallel to the y-axis, containing the local chordline at the collocation wing section y = constant and inclined to the onset flow and the $\hat{x}$-axis at an angle $\alpha + \alpha_T(y)$, where $\alpha_T(y)$ is the local twist angle, and assume that a singularity distribution on this plane produces the same velocity field - to second-order accuracy - at this collocation section, as would the same singularity distribution on the twisted chordal surface. Such an assumption has to be made here, since we intend to compute the perturbation velocity fields using the Ledger-Sells[3,4] computer subroutine which applies only to singularity distributions in a plane.

In extending the method, the effect of ground proximity can now be represented by planar image source and doublet singularities (of the same sign for sources, of opposite sign for doublets), and these can easily be incorporated

into the iterative scheme. As the Ledger-Sells subroutine can be used at any points off the plane containing the singularities, we can calculate the interference velocity fields induced on the wing by the image singularities, as well as by the basic chordal-surface singularities, and take them into account when we compute the residual errors R_t, R_ℓ in the boundary conditions. We expect that on the wing surface the interference fields will be small compared with the basic velocity fields, so that the residual errors will not be grossly increased (i.e. by an order of magnitude or more) and we can again cancel them approximately by adding suitable perturbation singularities as before, with unimpaired convergence. Thus no special modification is needed, even to the first set of singularity distributions, estimated from linear theory.

A further consequence of the comparative separation of the wing and its image is that the difference between the interference velocities on the upper and lower surfaces of a thin wing near a given point P on the wing chordal surface will be comparatively small, and so for moderate accuracy it will suffice to approximate to these on both surfaces by the values at one point only, say P, with a saving in computer time. The possible level of error due to this assumption is discussed, for a typical case, in section 4.

To compute the interference velocities, we need to know the coordinates of the points P relative to a local cartesian coordinate system (x',y,z') with origin in the image singularity plane corresponding to the section y = constant. We take the x'-axis parallel to the image of the local section chordline, and the z'-axis normal to it and in the general upward direction. We denote the ground clearance height of the local section trailing-edge T by $g_T(y,\alpha)$, so that the distance between T and its image T' is $2g_T$. An expression for $g_T(y,\alpha)$ is derived in the Appendix. The leading-edge image L' has the coordinates $(x' = x_L(y),\ y,\ z' = 0)$, and so T' has coordinates $(x_L(y) + c(y),\ y,\ 0)$. If the point P (usually referred to as a 'Weber point'[1]) has the local percentage-chord coordinate ξ, with $\xi = 0$ representing the leading-edge L, then the distance PT is $(1 - \xi)c(y)$. Referring to Fig.1, we can now write down the coordinates of P as:

$$\left[x_L + c + 2g_T \sin\alpha^* - (1 - \xi)c \cos 2\alpha^*,\ y,\ 2g_T \cos\alpha^* + (1 - \xi)c \sin 2\alpha^*\right]$$

where $\alpha^* = \alpha + \alpha_T(y)$.

The total interference velocity $\underline{u}_G$, due to sources and doublets, is computed as (u'_G, v'_G, w'_G) in the (x', y, z') system, and we need the components (u_G, v_G, w_G) in a local (x,y,z) system defined in the singularity plane containing the real local chordline, as in Ref.1. These are

$$u_G = u'_G \cos 2\alpha^* - w'_G \sin 2\alpha^*$$

$$v_G = v'_G$$

$$w_G = u'_G \sin 2\alpha^* + w'_G \cos 2\alpha^* \quad .$$

Since the interference velocity components do not change sign as we cross the wing chordal surface, the complete velocity field now has components (U,V,W) in the local (x,y,z) system, given on upper and lower surfaces (upper and lower signs respectively) by

$$U = (Q_0 + u_G) \pm Q_1$$

$$V = (Q_2 + v_G) \pm Q_3$$

$$W = (Q_5 + w_G) \pm Q_4$$

where Q_{0-5} are defined in equations (3-7) to (3-12) of Ref.1 for the wing out of ground effect.

3 SUCCESSIVE CALCULATION FOR SEVERAL AIRCRAFT HEIGHTS

It is convenient to be able to make calculations for several aircraft heights in one computer run. If the incidence and Mach number are held constant, the perturbation source and doublet distributions should not vary greatly as the height is varied, and so it should be practicable to use the distributions found iteratively for one height as a starting point for the next value of height. The corresponding velocity fields generated directly on the wing are still in store, and so the only preparatory work needed is the recalculation, at the new relative positions of wing and ground image, of the interference velocity field $\underline{u}_G$ due to the total source and doublet distributions corresponding to the previous height, which must of course be stored.

In this way we can save the major part of one iteration. So, having chosen (as input data) a number N_f of iterations judged necessary to secure acceptable accuracy, it seems reasonable to reduce N_f by one after completing the calculations for the first value of height, and this is now done by the program.

If the ratio of height above ground to semi-span is sufficiently large, the problem reduces to that of an isolated wing, and no calculations of $\underline{u}_G$ need be made. In the program, the value 100 of this ratio is judged sufficiently large.

4 RESULTS

4.1 RAE 100 section

As a first check on the method, we compare lift coefficients in two-dimensional flow, calculated for the 10% thick RAE 100 section, with some results obtained[5] by the panel method of Hess and Smith (AMOS)[6]. The section is given by[7]

$$\frac{Z_t}{c} = 0.148188\sqrt{\xi(1-\xi)}\left(1 - \frac{8}{9}\xi\right) \quad , \qquad \xi < 0.75,$$

$$\frac{Z_t}{c} = 0.0855564(1-\xi) \quad , \qquad \xi > 0.75.$$

To obtain a nearly two-dimensional flow without rewriting the program, this section was embodied in a rectangular wing with aspect ratio 60. Twelve chordwise collocation points were taken. For the two incidences $\alpha = \pm 5^\circ$ the section lift coefficient C_L is plotted against the reciprocal of the ratio of the height above ground h_Q (of the quarter chord point) to section chord c, in Fig.3. With this choice of abscissa we can include the results for the isolated wing, $c/h_Q = 0$, for which case the two methods agree well. For finite h_Q, differences appear; as h_Q/c decreases, the difference in C_L due to ground effect is at first overpredicted, then later underpredicted, by the present method relative to the AMOS method, the cross-over occurring at roughly $h_Q/c = 0.4$.

There are three possible reasons for these discrepancies. The first is that the difference in C_L due to ground effect may be relatively sensitive to

the level of accuracy with which the boundary conditions are satisfied. For the cases $h_Q/c = 0.75$ and 0.25, both at 5^o incidence, two sets of results are available, obtained using different first guesses while testing the program's option to deal with several heights consecutively. In the table below we show the numerically largest residual errors R_t, R_ℓ in the boundary conditions, and the corresponding values obtained for C_L . (The results with the smaller residual errors are the ones shown in Fig.3.) The number of iterations for these runs was $N_f = 2$.

h_Q/c	$R_{t_{max}}$	$R_{\ell_{max}}$	C_L
0.75	-0.0009	0.0018	0.6122
	0.0000	0.0003	0.6155
	AMOS		0.6007
0.25	-0.0068	0.0092	0.6537
	-0.0042	0.0054	0.6793
	AMOS		0.7058

As R_t and R_ℓ decrease, at $h_Q/c = 0.75$, C_L converges away from the AMOS value, but at $h_Q/c = 0.25$ it converges towards the AMOS value. In this latter case, extrapolating roughly to $R_t = 0$ gives $C_L = 0.7206$ while extrapolating to $R_\ell = 0$ gives $C_L = 0.7156$, so it is reasonable to assume that the final converged value lies somewhere in this range. In any event, the size of these differences for this level of accuracy in the boundary conditions, which would be quite reasonable for the wing out of ground effect, suggests that it may be worthwhile to ask for at least $N_f = 3$ iterations in general.

Another possible source of error is the approximation of equal interference velocities on upper and lower wing surfaces; to see by how much this approximation might be in error, the author computed, from two-dimensional formulae, the interference velocity fields due to the basic source and doublet distributions:

$$q_B = 2\frac{dz_t}{cdx} \quad , \qquad \ell_B = 4\alpha\sqrt{\frac{(1-\xi)}{\xi}} \quad .$$

He found that for the smallest height ratio $h_Q/c = 0.25$ and 5^o incidence, the difference in interference streamwash u_G on the upper and lower surfaces was typically about 25% of the mean interference streamwash and about 2% of the total streamwash. Which of these two numbers is more relevant is difficult to say, but (looking again at the table and comparing with the value 0.5810 of C_L for the section out of ground effect) we see that the error could be about 10% of the difference due to interference, and about 1% of the total. So it may be that for very accurate work the labour-saving assumption of equal interference velocities on upper and lower surfaces will have to be discarded, and the program revised accordingly.

The third possible source of error is just the discretization error due to the finite number of collocation points in either solution. However, the good agreement shown in Fig.3 for the section out of ground effect suggests that this error may be comparatively small, though it is unwise to draw any definite conclusion thereon without comparing the actual pressure distributions.

4.2 Finite wings

To demonstrate the program's performance on a finite wing, we present some results for two variants of a wing of 'airbus' type, the planform of which is shown in Fig.4. To get some idea of what happens at a wing tip comparatively near the ground one variant (denoted Var.1) is so chosen that, at incidence -0.05^o, the trailing-edge is everywhere at constant height g_T above the ground. When this constant height is about half the wing span ($g_T/s = 1.0$), there is little difference from the isolated wing condition. Figs.4 to 6 show what happens when g_T/s is decreased to 0.25 and then to 0.10. In this range, at the root and in mid-semispan the section lift (Fig.4) is increasing and we observe from the chordwise plots (Figs.5a-c) that the increase is due mainly to a change in the lower surface pressure distribution, the upper surface distribution changing comparatively little, so that (for this case) viscous effects due to boundary layer changes are likely to be small. This could not easily be predicted by a method for a thin wing, which takes no account of the interaction of thickness and ground effect, such as Maskew's[8]*. Near the tip, however, the section lift starts to decrease somewhere between $g_T/s = 0.25$ and 0.10; there is clearly a further three-dimensional effect outboard, and the detailed computer output shows that the induced incidence (due to interference) is decreasing in this

* In the present method, even though the perturbation due to the ground is taken to be the same on both surfaces, the effect on C_p of compounding the velocity vectors is not the same.

region, as the ground clearance is reduced. The local spanwise centre of pressure plot (Fig.6) tells us also that the overall centre of pressure moves forward as the ground clearance decreases, which could imply an unfavourable nose-up pitching moment (for this hypothetical case).

To demonstrate the ability of the program to handle wings in which the trailing-edge ground clearance is not constant along the span, we consider another variant (denoted Var.2) of this wing in which the ground clearance ratio (at $\alpha = -0.05^{o}$) varies linearly from 0.10 at the root to 0.05 at the tip. In Figs.7 and 8 the spanwise lift distribution and centre of pressure locus are shown for Var.2, and also for Var.1 with $g_T/s = 0.10$ and with $g_T/s = 0.05$, as before. As one might expect, the results for Var.2 agree with the results for Var.1 at $g_T/s = 0.10$ inboard, and with the other set outboard. Incidentally, the trend towards loss of lift with decreasing ground clearance has spread inboard to the root, as we expect to happen in due course from two-dimensional studies (Küchemann[9]).

No quantitative conclusions are drawn from these results, for two reasons. Firstly, the problem is somewhat academic; secondly, the differences shown might be comparable with the computational errors discussed earlier with the results for the two-dimensional section, though if these errors are assumed to be similar for all runs, which in this case all started from the same initial conditions, the qualitative comparisons above are still likely to be sensible.

5 CONCLUSION

The method of chordal-surface singularities for calculating flow past an isolated wing, proposed by Weber[2] and implemented by Sells[1], has been extended to cover the case of a wing in ground effect.

By taking advantage of the comparatively small size of the interference velocity fields, we have avoided extensive changes to the basic program; moreover, computing times are not greatly increased, though results for a two-dimensional section suggest that the pressure distribution and section lift may be more sensitive to the residual errors in the wing boundary conditions than in the isolated-wing problem, so that at least one more iteration may be advisable. Since the basic program requires at least two iterations, this implies that for the same accuracy the new program ought to be run for at least three.

The inclusion of the effect of wing thickness, as well as those of camber, twist and incidence, on the surface pressure distributions, by allowing a better prediction of boundary-layer effects, may serve to fill a gap in current numerical technique for this problem. As an example of this hypothesis, we show results for a case in which we can deduce that viscous effects are probably similar to those for the wing in free air.

Appendix

THE LOCAL TRAILING-EDGE GROUND CLEARANCE

In order to compute the interference velocities induced on the wing by the image singularities, we need some information about the ground clearance. Since the wing trailing-edge is frequently made up of straight line segments, and is generally nearer than the leading-edge to the ground, it seems reasonable to work with trailing-edge ordinates.

We input, as part of the flow field data, the height (ground clearance) h_T of the section trailing-edge T_0 at the root $y = 0$. As part of the data specifying the wing geometry we input the spanwise variation $\hat{z}_T(y)$ of the height of the local trailing-edge T_y above the root trailing-edge T_0 in the reference configuration of zero incidence, $\alpha = 0$; see Fig.2, in which T_y has been projected onto the root plane $y = 0$, which is the plane of the paper. Knowing the local leading-edge ordinate $x_L(y)$ and chord $c(y)$, we can write down the horizontal separation $\hat{x}_t(y)$ of T_0 and T_y in the reference configuration:

$$\hat{x}_T(y) = x_L(y) + c(y) - x_L(0) - c(0) \quad .$$

We also have the angle θ between T_0T_y and the x-axis, defined by

$$\tan \theta = \hat{z}_T/\hat{x}_T \quad .$$

At incidence α, the line T_0T_y rotates to T_0T where T is the new projection of the local trailing-edge on $y = 0$. Then the total ground clearance $g_T(y,\alpha)$ of the local trailing-edge is the algebraic sum of the root ground clearance and the vertical separation between T_0 and T :

$$g_T(y,\alpha) = h_T + \left(\hat{x}_T^2 + \hat{z}_T^2\right)^{\frac{1}{2}} \sin(\theta - \alpha)$$

$$= h_T + \hat{z}_T(y) \cos\alpha - \hat{x}_T(y) \sin\alpha \quad .$$

SYMBOLS

$c(y)$	chord
C_L	two-dimensional section lift coefficient
$C_{LL}(y)$	local section lift coefficient
$g_T(y,\alpha)$	height above ground of trailing-edge of wing section in y = constant at incidence α
h_T	height above ground of wing-root trailing-edge
h_Q	height above ground of quarter-chord point
N_f	number of iterations
R_t, R_ℓ	residual errors in symmetrical and antisymmetrical wing boundary conditions
$\underline{u}_G$	interference velocity (induced on wing by ground image singularities)
u_G, v_G, w_G	components of $\underline{u}_G$ in (x,y,z)-axes
u'_G, v'_G, w'_G	components of $\underline{u}_G$ in (x',y,z')-axes
U, V, W	total-velocity components
x, y, z	axes in plane of wing chordline
x', y, z'	axes in plane of image chordline
$\hat{x}$, y, $\hat{z}$	free-stream axes, centred on wing-root trailing-edge
$x_L(y)$	leading-edge ordinate
z_t	wing thickness
α	angle of incidence
$\alpha_T(y)$	local twist angle
α^*	$\alpha + \alpha_T$

REFERENCES

No.	Author	Title, etc.
1	C.C.L. Sells	Iterative method for thick cambered wings in subcritical flow. ARC R & M 3786 (1974)
2	J. Weber	Second-order small-perturbation theory for finite wings in incompressible flow. ARC R & M 3759 (1972)
3	J.A. Ledger	Computation of the velocity field induced by a planar source distribution approximating a symmetrical, non-lifting wing in subsonic flow. ARC R & M 3751 (1972)
4	C.C.L. Sells	Calculation of the induced velocity field on and off the wing plane for a swept wing with given load distribution. ARC R & M 3725 (1970)
5	D.N. Foster	Private communication
6	J.L. Hess A.M.O. Smith	Calculation of potential flow about arbitrary bodies. *Progress in Aeron. Scs.* 8, pp.1-138, Pergamon Press (1967)
7	R.C. Pankhurst H.B. Squire	Calculated pressure distributions for the RAE 100-104 aerofoil sections. ARC CP No.80 (1950)
8	B. Maskew	On the influence of camber and non-planar vortex wake on wing characteristics in ground effect. ARC CP No.1264 (1971)
9	D. Küchemann	The aerodynamic design of aircraft - an introduction (Part 4). MOD(PE) unpublished work

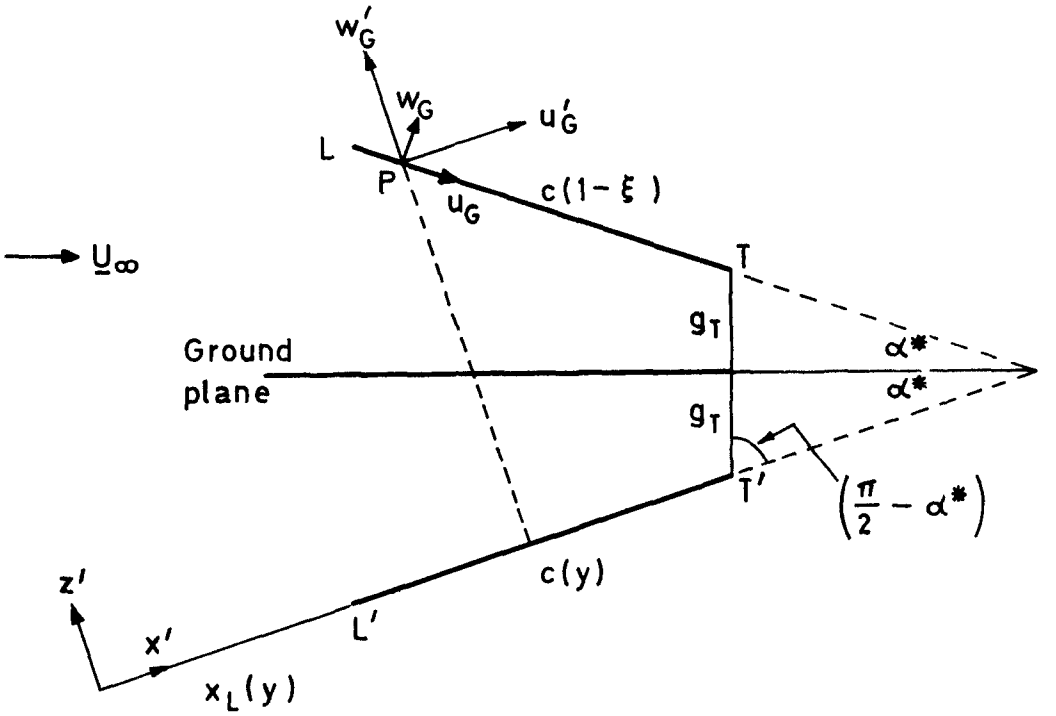

Fig.1 The chordline, and its ground image, in a plane y = constant

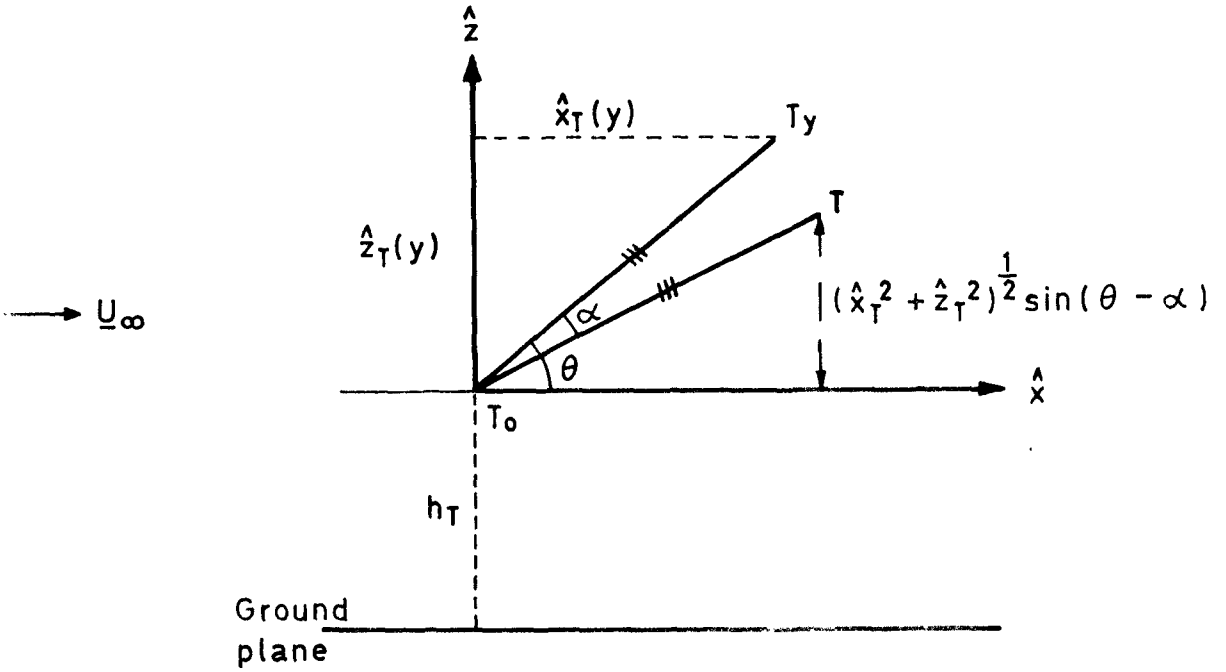

Fig.2 The local trailing-edge ground clearance

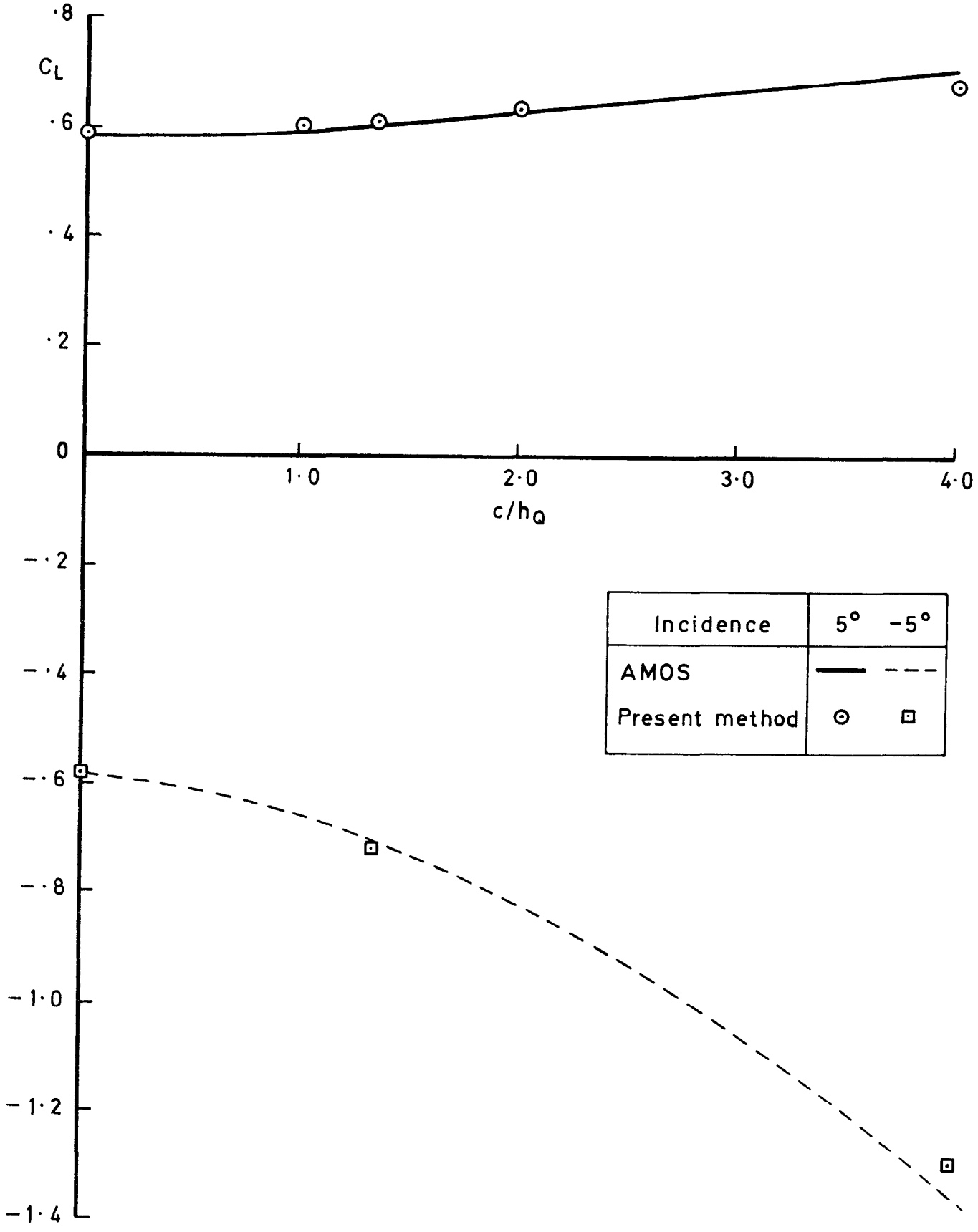

Fig. 3 Variation of lift coefficient with height above ground at fixed incidence 10% RAE 100 section

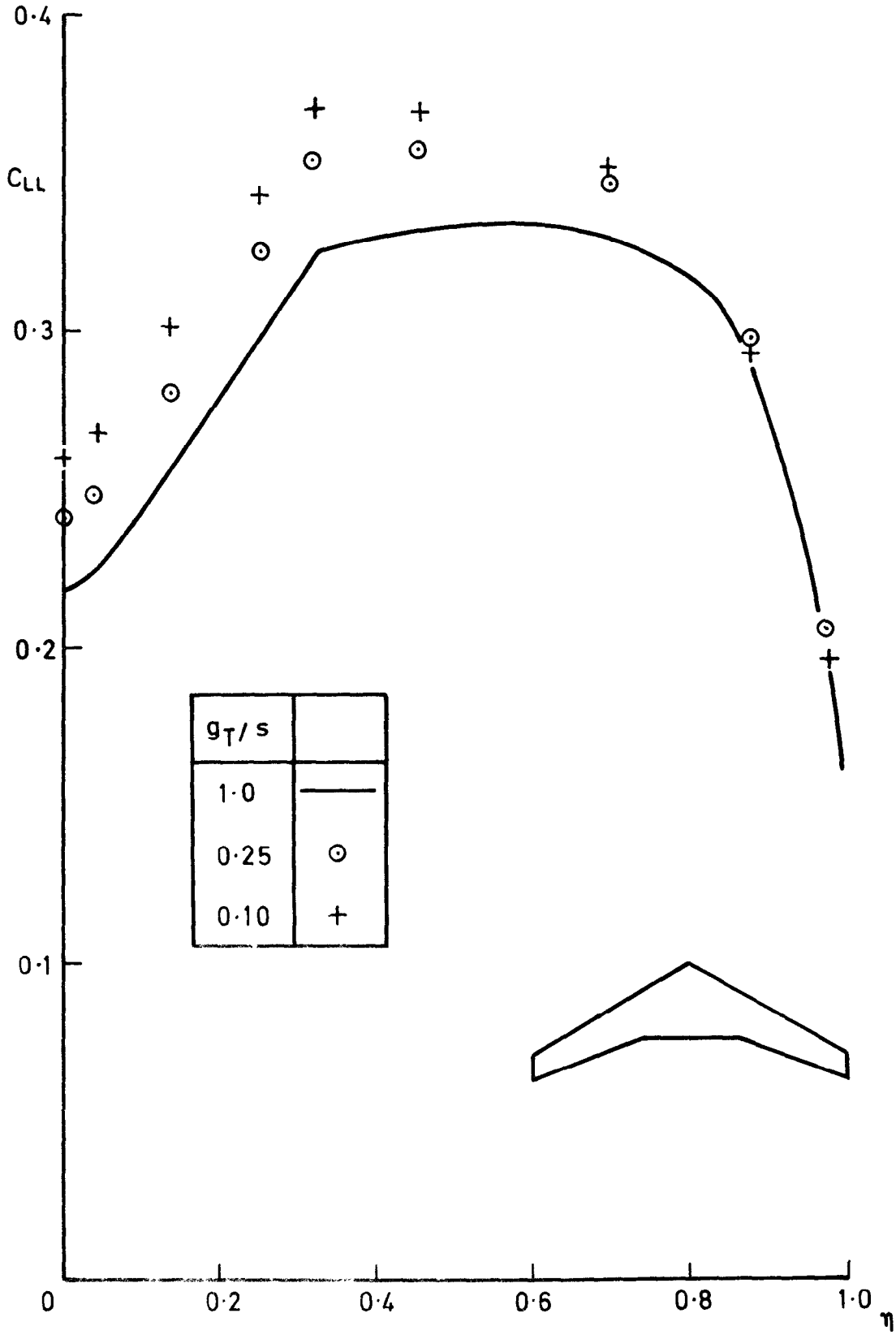

Fig.4 Effect of height above ground on spanwise lift distribution. Modified airbus wing, $\alpha = -0{\cdot}05°$

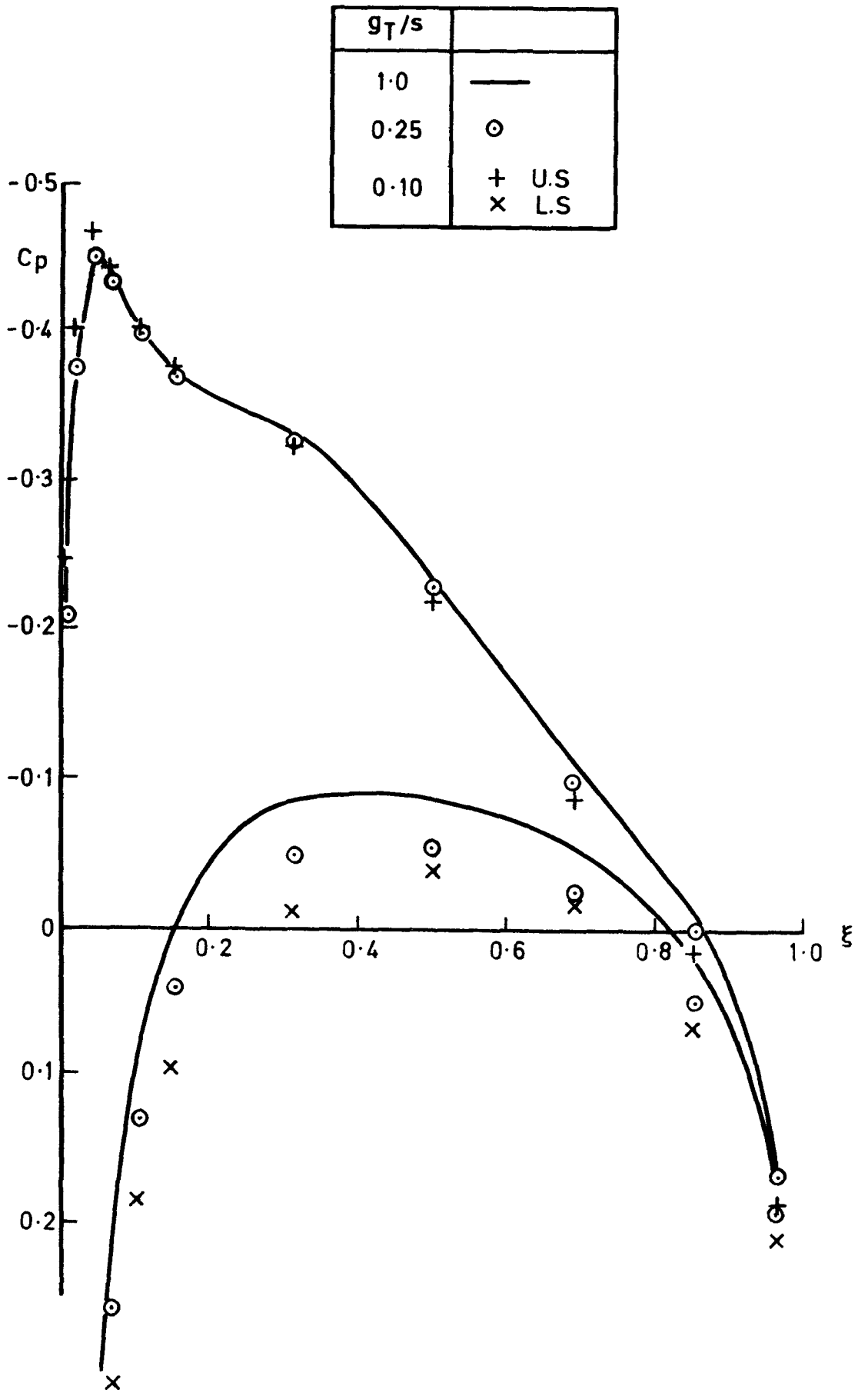

Fig.5a Effect of height above ground on chordwise pressure distribution:(a) $\eta = 0$. 'Airbus' type wing (Var.1), $\alpha = -0{\cdot}05°$

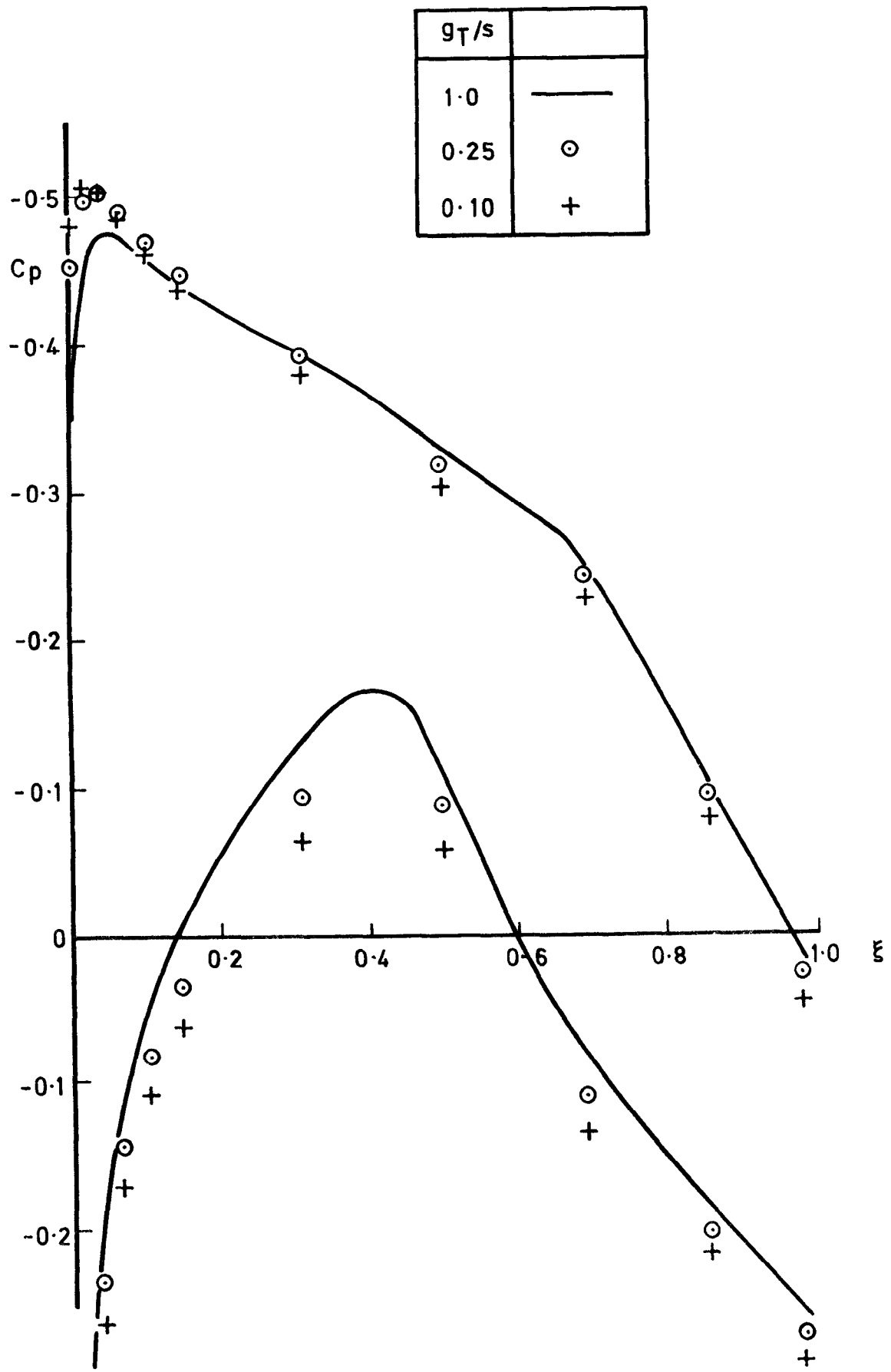

Fig.5b Effect of height above ground on chordwise pressure distribution: (b) $\eta = \cdot 46$. 'Airbus' type wing (Var.1), $\alpha = -0 \cdot 05°$

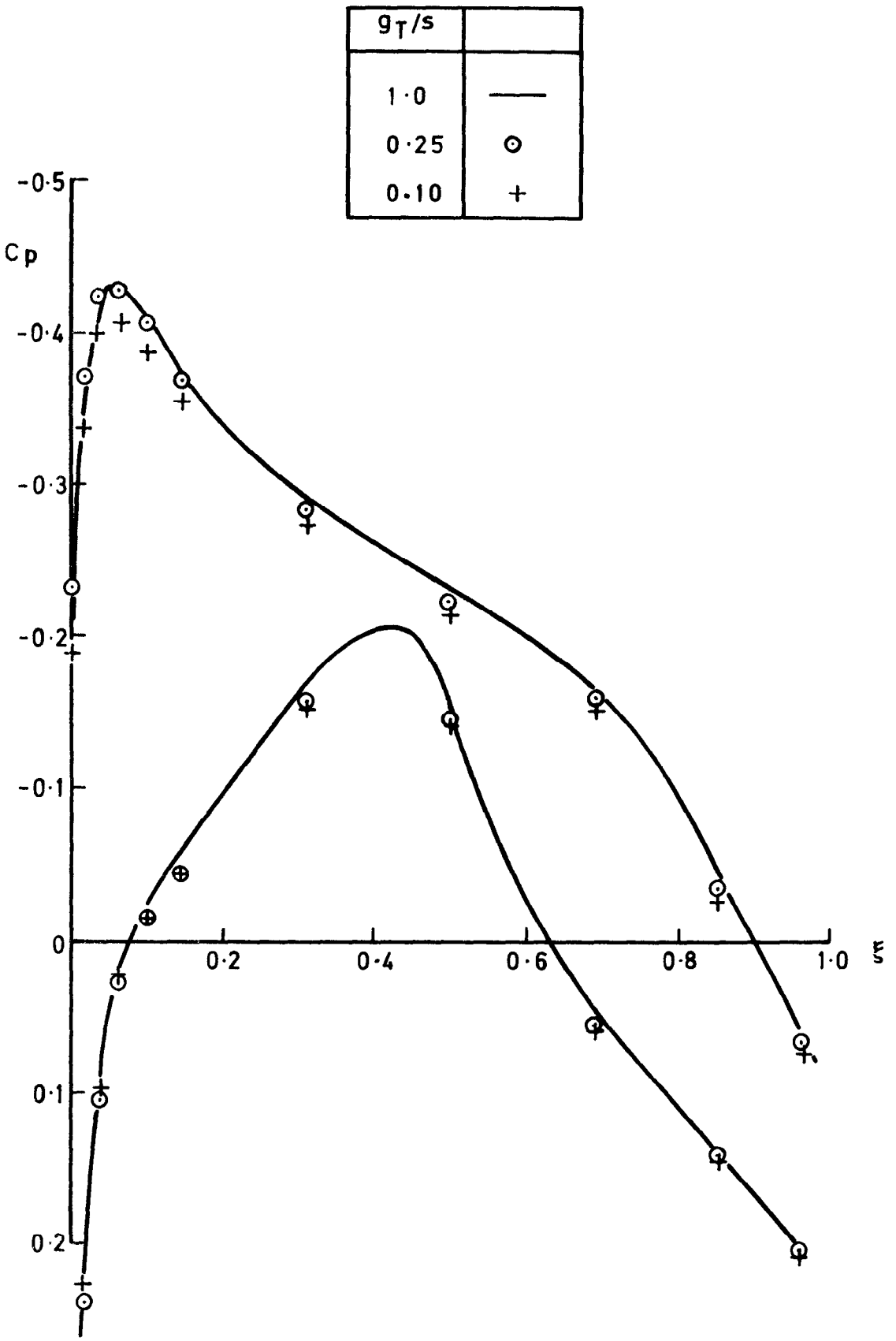

Fig.5c Effect of height above ground on chordwise pressure distribution: (c) $\eta = \cdot 97$. 'Airbus' type wing (Var.1), $\alpha = -0 \cdot 05°$

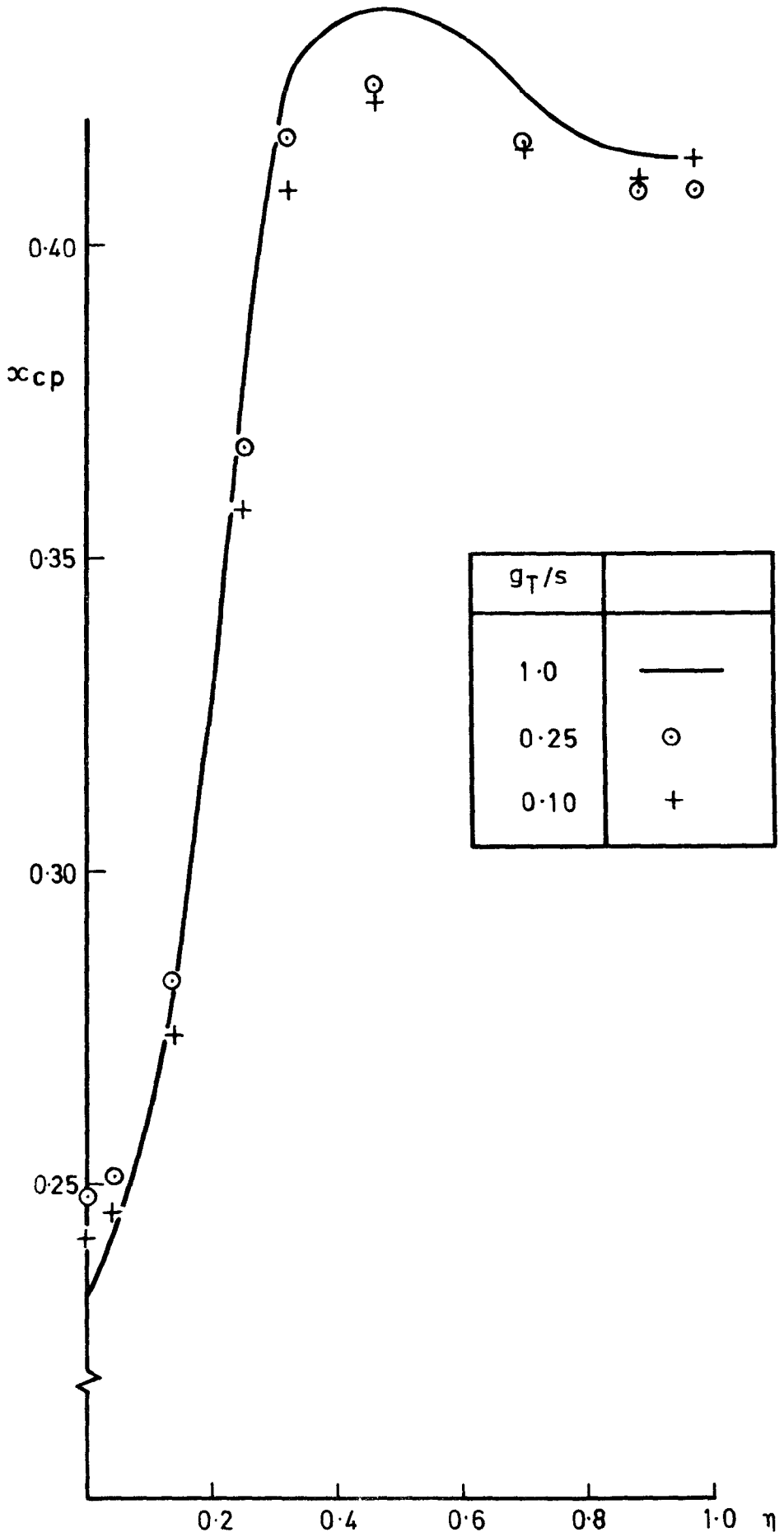

Fig.6 Effect of height above ground on local centre of pressure. Airbus type wing (Var.1), $\alpha = -0{\cdot}05°$

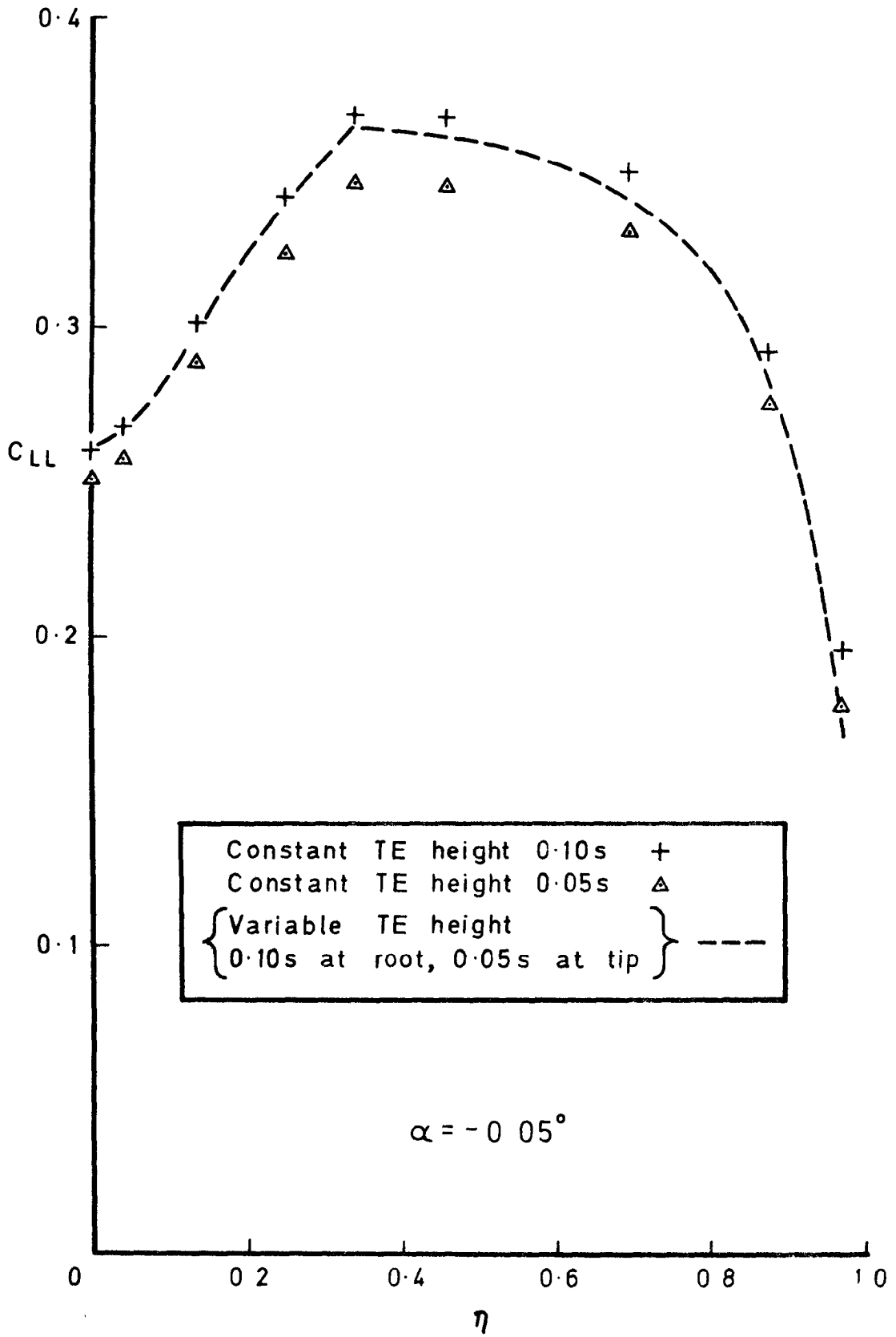

Fig.7 Effect of different trailing edge height configurations on spanwise lift distribution

ARC CP No.1370
April 1976

Sells, C. C. L.

533.69.01
533.6.044.7
533.6.043.1
533.682
533.6.011.32

ITERATIVE CALCULATION OF FLOW PAST A THICK CAMBERED WING NEAR THE GROUND

The author's method to compute the steady low-speed inviscid flow past a wing in free air, is extended to take account of ground effect. The basic method represents the perturbation due to the wing by iteratively computed distributions of sources and doublets on the wing chordal surface, at each iteration the ground effect is represented by the images in the ground plane of these distributions, the strengths of which are calculated from the computed errors in the boundary conditions on upper and lower surfaces. For a given angle of incidence (and Mach number), several heights above the ground in succession can be treated, with some economy in computing time.

Results are presented for a two-dimensional section (RAE 100) and for two variants of a wing of 'airbus' type. Comparisons with another method for the RAE 100 section suggest that the present method generally needs at least three iterations, and that for very accurate results at low ground heights further work on the program is needed.

ARC CP No 1370
April 1976

Sells, C. C L.

533.69.01 :
533.6.044.7 :
533.6.043.1 :
533.682 :
533.6.011.32

ITERATIVE CALCULATION OF FLOW PAST A THICK CAMBERED WING NEAR THE GROUND

The author's method to compute the steady low-speed inviscid flow past a wing in free air, is extended to take account of ground effect. The basic method represents the perturbation due to the wing by iteratively computed distributions of sources and doublets on the wing chordal surface; at each iteration the ground effect is represented by the images in the ground plane of these distributions, the strengths of which are calculated from the computed errors in the boundary conditions on upper and lower surfaces. For a given angle of incidence (and Mach number), several heights above the ground in succession can be treated, with some economy in computing time.

Results are presented for a two-dimensional section (RAE 100) and for two variants of a wing of 'airbus' type. Comparisons with another method for the RAE 100 section suggest that the present method generally needs at least three iterations, and that for very accurate results at low ground heights further work on the program is needed.

Cut here

ARC CP No.1370
April 1976

Sells, C. C. L.

533.69.01 :
533.6.044.7 :
533.6.043.1 :
533.682 :
533.6.011.32

ITERATIVE CALCULATION OF FLOW PAST A THICK CAMBERED WING NEAR THE GROUND

The author's method to compute the steady low-speed inviscid flow past a wing in free air, is extended to take account of ground effect. The basic method represents the perturbation due to the wing by iteratively computed distributions of sources and doublets on the wing chordal surface; at each iteration the ground effect is represented by the images in the ground plane of these distributions, the strengths of which are calculated from the computed errors in the boundary conditions on upper and lower surfaces. For a given angle of incidence (and Mach number), several heights above the ground in succession can be treated, with some economy in computing time.

Results are presented for a two-dimensional section (RAE 100) and for two variants of a wing of 'airbus' type. Comparisons with another method for the RAE 100 section suggest that the present method generally needs at least three iterations, and that for very accurate results at low ground heights further work on the program is needed.

Cut here

DETACHABLE ABSTRACT CARDS

DETACHABLE ABSTRACT CARDS

Published by
HER MAJESTY'S STATIONERY OFFICE

Government Bookshops
49 High Holborn, London WC1V 6HB
13a Castle Street, Edinburgh EH2 3AR
41 The Hayes, Cardiff CF1 1JW
Brazennose Street, Manchester M60 8AS
Southey House, Wine Street, Bristol BS1 2BQ
258 Broad Street, Birmingham B1 2HE
80 Chichester Street, Belfast BT1 4JY
Government Publications are also available through booksellers

C.P. No. 1370

ISBN 011 471116 X